AIP | Applied Physics Letters

Effects of Nb doping level on the electronic transport, photoelectric effect and magnetoresistance across La0.5Ca0.5MnO3/Nb:SrTiO3 junctions

J. F. Wang, Y. C. Jiang, M. G. Chen, and J. Gao

Citation: Applied Physics Letters **103**, 252103 (2013); doi: 10.1063/1.4851076
View online: http://dx.doi.org/10.1063/1.4851076
View Table of Contents: http://scitation.aip.org/content/aip/journal/apl/103/25?ver=pdfcov
Published by the AIP Publishing

Articles you may be interested in

Electric transport and field-induced properties in ZnO/La0.4Gd0.1Sr0.5CoO3/Si heterostructure
J. Appl. Phys. **114**, 133705 (2013); 10.1063/1.4823777

Temperature-dependent transport and transient photovoltaic properties of La2/3Ca1/3MnO3/Nb:SrTiO3 heteroepitaxial p-n junction
J. Appl. Phys. **112**, 023101 (2012); 10.1063/1.4737256

Buffer-layer-enhanced magnetic field effect in La0.5Ca0.5MnO3/LaMnO3/SrTiO3:Nb heterojunctions
J. Appl. Phys. **109**, 07C729 (2011); 10.1063/1.3562916

Bias-dependent rectifying properties of n - n manganite heterojunctions La 1 − x Ca x MnO 3 / SrTiO 3 : Nb (x = 0.65 – 1)
Appl. Phys. Lett. **93**, 212502 (2008); 10.1063/1.3021399

Disorder effects in (LaTb) 0.5 (CaSr) 0.5 MnO 3 compounds
J. Appl. Phys. **95**, 7097 (2004); 10.1063/1.1687257

HIDEN ANALYTICAL
Instruments for Advanced Science

Contact Hiden Analytical for further details:
W www.HidenAnalytical.com
E info@hiden.co.uk
CLICK TO VIEW our product catalogue

Gas Analysis
- dynamic measurement of reaction gas streams
- catalysis and thermal analysis
- molecular beam studies
- dissolved species probes
- fermentation, environmental and ecological studies

Surface Science
- UHV TPD
- SIMS
- end point detection in ion beam etch
- elemental imaging - surface mapping

Plasma Diagnostics
- plasma source characterization etch and deposition process reaction
- kinetic studies
- analysis of neutral and radical species

Vacuum Analysis
- partial pressure measurement and control of process gases
- reactive sputter process control
- vacuum diagnostics
- vacuum coating process monitoring

This article is copyrighted as indicated in the article. Reuse of AIP content is subject to the terms at: http://scitation.aip.org/termsconditions. Downloaded to IP: 147.8.204.164 On: Wed, 25 Feb 2015 10:00:36

APPLIED PHYSICS LETTERS **103**, 252103 (2013)

Effects of Nb doping level on the electronic transport, photoelectric effect and magnetoresistance across $La_{0.5}Ca_{0.5}MnO_3$/Nb:$SrTiO_3$ junctions

J. F. Wang,[1,2,a)] Y. C. Jiang,[1] M. G. Chen,[2] and J. Gao[1,b)]
[1]*Department of Physics, The University of Hong Kong, Pokfulam Road, Hong Kong*
[2]*College of Science, China Jiliang University, Hangzhou, Zhejiang 310018, People's Republic of China*

(Received 29 October 2013; accepted 3 December 2013; published online 16 December 2013)

Heterojunctions composed of $La_{0.5}Ca_{0.5}MnO_3$ and Nb doped $SrTiO_3$ were fabricated, and the effects of the Nb doping level on their electronic transport, photoelectric effect, and magnetoresistance were investigated. A lower doping concentration of Nb led to better rectifying properties and higher open circuit voltages. The *I-V* curves for $La_{0.5}Ca_{0.5}MnO_3$/0.7 wt. % Nb-$SrTiO_3$ showed a negligible response to magnetic fields for all temperatures, whereas $La_{0.5}Ca_{0.5}MnO_3$/0.05 wt. % Nb-$SrTiO_3$ exhibited distinct magnetoresistance, which depended on both the bias voltage and temperature. These results are discussed with the assistance of conventional semiconductor theories. © *2013 AIP Publishing LLC*.
[http://dx.doi.org/10.1063/1.4851076]

Oxide heterostructures have received much attention in recent years.[1–4] For semiconductor heterojunctions, although the charge density is the only modulated parameter, they exhibit many striking properties.[5] For heterostructures constructed with complex oxides, more parameters, such as exchange energies and hopping energies, could be tuned at the interfaces.[1] As a result, more prominent properties that are absent in bulk materials might emerge with these structures.

Perovskite manganites, which show unexpected sensitivity to applied magnetic fields, light, electric currents/fields, and pressure, are typical strongly correlated complex oxides.[6–8] Heterostructures composed of manganites and doped strontium titanate have been intensively studied.[9–19] In 1999, Sugiura *et al.* reported good rectifying properties in $La_{0.85}Sr_{0.15}MnO_3$/i-$SrTiO_3$/$La_{0.05}Sr_{0.95}TiO_3$ junctions.[9] Following studies indicate that a single-interface junction can be fabricated by growing a manganite film on a doped $SrTiO_3$ substrate. In such junctions, highly rectifying current-voltage characteristics, magnetocapacitance, bias-tunable magnetoresistance, and magnetic-field tunable photo voltages have been demonstrated.[10–14] However, the understanding of these junctions is still limited. It is hindered by strong correlations in the manganites.[6–8] The behavior of these junctions may be influenced by extrinsic factors, such as leakage currents.[20] The doping level is an intrinsic parameter that can affect their properties, and its effect in these junctions has not been investigated. In this study, we examine the effects of the Nb doping level on the electronic transport, photoelectric effect, and magnetoresistance in $La_{0.5}Ca_{0.5}MnO_3$/x wt. % Nb ($x = 0.7$ and 0.05) doped $SrTiO_3$ junctions (denoted as LCMO/0.7Nb-STO and LCMO/0.05Nb-STO, respectively). $La_{0.5}Ca_{0.5}MnO_3$ displays many intriguing properties, such as charge ordering and orbital ordering. The study on $La_{0.5}Ca_{0.5}MnO_3$/Nb-$SrTiO_3$ junctions could provide a reference for similar heterojunctions constructed with half-doped manganites. It is found that the doping level of Nb significantly altered the behaviors of these junctions.

LCMO (60 nm) films were deposited on 0.7 wt. % and 0.05 wt. % (001)-oriented Nb-STO by using pulsed laser ablation. The fabrication conditions can be found in Ref. 16. Junctions with an area of ~1 × 1 mm^2 were formed by using a photolithography technique to define the pattern and hydrogen chloride (HCl)-potassium iodide (KI) etchant to remove the uncovered LCMO. Ohmic contacts were formed by evaporating sliver (Ag) films onto LCMO and Nb-STO (see the inset in Fig. 1). All transport properties were measured with a two-probe configuration, and the positive voltage applied on LCMO was defined as the forward bias. For the magnetoresistance (MR) measurements, the magnetic fields were applied normal to the film plane.

X-ray diffraction (XRD) measurements indicate that the LCMO films are epitaxially c-axis oriented. Figure 1 shows a typical θ-2θ XRD pattern for the LCMO/Nb-STO structures. Only the reflection peaks from the (00l) planes for LCMO (for LCMO the pseudocubic index is used) and Nb-STO can be observed. The out-of-plane lattice constant of the LCMO film, calculated from the reflection peak, is $c \sim 3.772$ Å, indicating a compressive out-of-plane strain. Because the lattice constant in the bulk LCMO ($a_p \sim 3.827$ Å) is smaller than that of

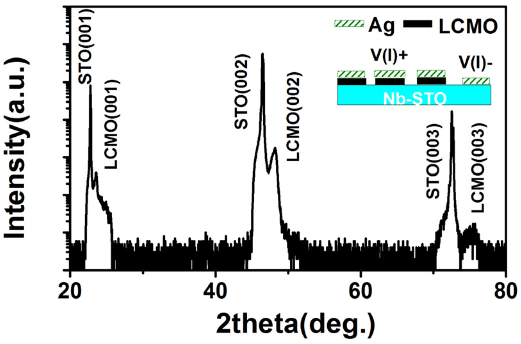

FIG. 1. A typical XRD pattern (θ-2θ scan) of LCMO/Nb-STO. Shown in the inset is the schematic view of the junction.

[a)] Electronic mail: jifewang@gmail.com

[b)] Author to whom correspondence should be addressed. Electronic mail: jugao@hku.hk.

Nb-STO ($a \sim 3.905$ Å), the LCMO films grown on Nb-STO should experience a tensile in-plane strain and a compressive out-of-plane strain. It is noted that the change in the Nb doping level from $x = 0.05$ to 0.7 has a negligible influence on the lattice constant of STO and the strain states in the LCMO films. Therefore, strain should play a paltry role in the differences in the properties of these junctions.

Figure 2 displays the current-voltage curves for LCMO/0.7Nb-STO and LCMO/0.05 Nb-STO at 300 K. For both junctions, there was a clear asymmetry between the forward and the reverse biases. As compared to that under the negative voltage, the current under the positive bias began to increase at lower voltages. One significant difference was that the rectifying properties in LCMO/0.05Nb-STO were much better than those in LCMO/0.7Nb-STO. For LCMO/0.05Nb-STO, the backward current was less than 1 μA, even for a voltage of -5 V. In contrast, the reverse current in LCMO/0.7Nb-STO reached 1 mA at ~ -1 V.

Figures 3(a) and 3(b) display the forward J-V curves recorded at different temperatures for LCMO/0.7Nb-STO and LCMO/0.05 Nb-STO, respectively. There were clear differences for these two junctions. At a selected temperature, the forward current in LCMO/0.7Nb-STO began to rise at lower voltages and increased much more slowly. For both junctions, above 100 K, in a certain intermediate current range, log$J$ changed linearly with V. In such a circumstance, it is possible to use semiconductor theory to analyze these junctions. For either the Schottky junction model or the p-n junction model, the J-V relation in the forward direction can be expressed as $J \approx J_S \exp(qV/nk_BT)$ when $qV \gg k_BT$, where J_S is the saturation current density, n the ideality factor, and k_B the Boltzmann constant. The deduced values of J_S, q/nk_BT, and n at different temperatures are shown in Figs. 3(c)–3(e), respectively. For both junctions, with a decrease in the temperature, J_S was reduced, and n was increased. At all temperatures, the J_S and n in LCMO/0.05Nb-STO were smaller than those in LCMO/0.7Nb-STO. For a Schottky junction with a purely thermal emission process or a p-n junction with only a diffusion process, n is 1. For LCMO/0.05Nb-STO, at 300 K n was $\sim$1.1. This indicates that at room temperature the thermal process or the diffusion process dominates in these junctions. The deviation from unity may be caused by several factors. One is the strong correlation in manganites, which may cause junction inhomogeneity. Because these two junctions have identical layer of LCMO, strong correlation in manganites cannot explain the difference between them. Another possibility is the involvement of other transport processes, such as tunneling. The increase in n with a decreasing temperature in LCMO/0.05Nb-STO is probably due to the increased contribution of the tunneling currents at low temperatures.[16,19,20] Tunneling also becomes more significant with an increasing doping level because the square of the barrier width W^2 is proportional to $1/N$, where N is the carrier concentration (doping level).[5] For direct tunneling, the slope of the ln$J$-V curve is independent of temperature. This explains why in LCMO/0.7Nb-STO the deduced slope q/nk_BT showed a much weaker temperature dependence.

Figure 4 depicts the responses of the I-V curves to light illumination. A semiconductor laser diode (wavelength = 532 nm and power density = 2 mW/mm^2) was used as the light source. Both junctions showed clear changes under light irradiation. The short circuit current (I_{SC}) in LCMO/0.7Nb-STO was slightly larger than that in LCMO/0.05Nb-STO. This is reasonable and consistent with the previous report.[21] A higher doping level leads to a narrower depletion width and a lower built-in potential.[5]

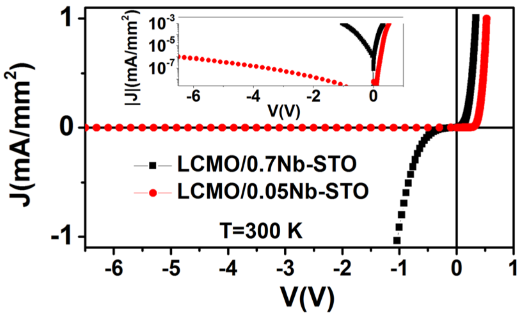

FIG. 2. J vs V curves for LCMO/0.7Nb-STO and LCMO/0.05 Nb-STO measured at 300 K.

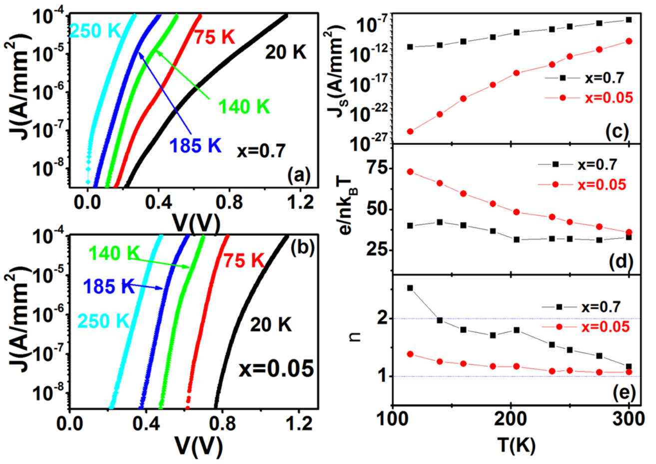

FIG. 3. Forward J-V curves measured at 250, 185, 140, 75, and 20 K for LCMO/0.7Nb-STO (a) and LCMO/0.05 Nb-STO (b). J_S (c), $e/(nk_BT)$ (d) and n (e) as a function of temperature.

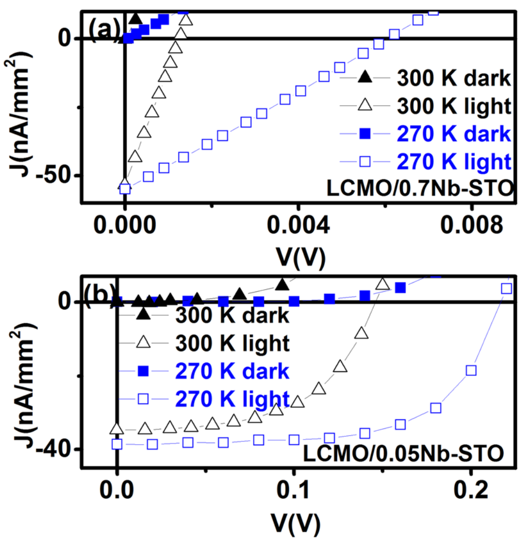

FIG. 4. J-V curves with and without light ($\lambda = 532$ nm, $P = 2$ mW/mm^2) at 300 K and 270 K for LCMO/0.7Nb-STO (a) and LCMO/0.05 Nb-STO (b).

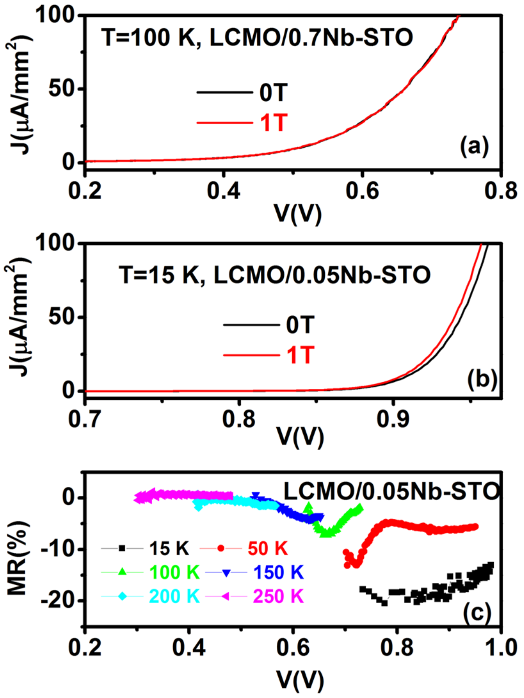

FIG. 5. (a) Forward *J-V* curve with and without a magnetic field of 1 T at 100 K for LCMO/0.7Nb-STO; (b) Forward *J-V* curve with and without a magnetic field of 1 T at 15 K for LCMO/0.05Nb-STO; (c) Bias dependent *MR* at 250, 200, 150, 100, 50, and 15 K for LCMO/0.05 Nb-STO. At each temperature, the *MR* is calculated using $MR(V) = 100\% \times [R(V, 1T)\text{-}R(V, 0T)]/R(V, 0T)$ when the current is in the range of 10^{-7} A to 10^{-4} A.

Internal photoemission spectroscopy experiments on $SrRuO_3$/Nb-doped $SrTiO_3$ junctions revealed that the junction constructed with a heavier Nb doping had a slightly lower Schottky barrier height and a slightly larger photo yield in the energy range of 1.3–2.4 eV.[21] The largely reduced open circuit voltage (V_{OC}) in LCMO/0.7Nb-STO should be a combined consequence of the lowering in upper limit of V_{OC} and the tremendous increase in J_S. A slight reduction in barrier height lowered the upper limit of the V_{OC}. For conventional p-n junctions and Schottky junctions, V_{OC} depends on J_S, $V_{OC} \sim k_BTln(J_L/J_S)/e$,[5] where J_L is the photocurrent density. Both the decrease of the barrier height and the reduction of depletion length lead to the increase of J_S. As shown in Fig. 3(c), the change of the Nb doping concentration from 0.05 to 0.7 increased J_S by almost 3 orders at room temperature. Consequently, V_{OC} was suppressed greatly.

Intriguingly, the doping level of Nb in STO also affected the response to magnetic fields in the junctions. For LCMO/0.7Nb-STO, at all temperatures, a magnetic field of 1 T had negligible effects on the *J-V* curves [see Fig. 5(a)]. On the contrary, for LCMO/0.05Nb-STO, clear responses of the *J-V* curves to magnetic fields were observed, as shown in Fig. 5(b). With the definition $MR(V) = 100\% \times [R(V, 1T)\text{-}R(V, 0T)]/R(V, 0T)$, the *MR*s at various temperatures are summarized in Fig. 5(c). *MR* exhibited complex behaviors. At a fixed temperature, with the increase in the bias voltage, *MR* first rose and then fell. When the temperature was lowered, the maximum *MR* increased continuously. The *MR* observed in LCMO/0.05Nb-STO cannot be attributed to the *MR* in LCMO because LCMO/0.7Nb-STO did not exhibit *MR*. We calculated the junction resistance $R_j(=V/I)$ at various bias voltages. Over the whole voltage range, R_j dropped quickly as the bias voltage was increased. This indicates that the main voltage drop occurred at the junction. Otherwise, the resistance would be almost constant with an increasing bias voltage. Therefore, the *MR* observed in LCMO/0.05Nb-STO cannot be attributed to the *MR* in LCMO. The differences in the responses to the magnetic fields for LCMO/0.05Nb-STO and LCMO/0.7Nb-STO are likely caused by their different transport mechanisms. Further studies are required to gain a complete understanding of the magnetic field responses in these junctions.

In summary, LCMO/Nb-STO heterojunctions were fabricated by pulsed laser deposition, and the effects of the Nb doping level were examined. XRD spectra revealed a good epitaxy between the LCMO films and the Nb-STO substrates. Junctions constructed with the low doped substrates exhibited better rectifying properties and larger open circuit voltages. The increase in the Nb doping level slightly enhanced the short circuit currents. Analysis using conventional semiconductor theory indicates that a higher doping level of Nb resulted in a narrow barrier width and a high saturation current density. The responses to magnetic fields in these junctions also depended on the doping level of Nb in STO.

This work has been supported by Grants of the Research Grant Council of Hong Kong (Project No. HKU 701813P), the Natural Science Foundation of China (Project Nos. 11374225 and 11304298) and Zhejiang Provincial Natural Science Foundation (Grant No. LQ13A040002).

[1] J. Mannhart and D. G. Schlom, Science **327**, 1607 (2010).
[2] H. Takagi and H. Y. Hwang, Science **327**, 1601 (2010).
[3] J. S. Lee, Y. W. Xie, H. K. Sato, C. Bell, Y. Hikita, H. Y. Hwang, and C. C. Kao, Nature Mater. **12**, 703 (2013).
[4] G. Berner, M. Sing, H. Fujiwara, A. Yasui, Y. Saitoh, A. Yamasaki, Y. Nishitani, A. Sekiyama, N. Pavlenko, T. Kopp, C. Richter, J. Mannhart, S. Suga, and R. Claessen, Phys. Rev. Lett. **110**, 247601 (2013).
[5] S. M. Sze and K. K. Ng, *Physics of Semiconductor Devices*, 3rd ed. (John Wiley & Sons, Inc., Hoboken, New Jersey, 2006).
[6] E. Dagotto, T. Hotta, and A. Moreo, Phys. Rep. **344**, 1 (2001).
[7] M. B. Salamon and M. Jaime, Rev. Mod. Phys. **73**, 583 (2001).
[8] Y. Tokura, Rep. Prog. Phys. **69**, 797 (2006).
[9] M. Sugiura, K. Uragou, M. Noda, M. Tachiki, and T. Kobayashi, Jpn. J. Appl. Phys., Part 1 **38**, 2675 (1999).
[10] F. M. Postma, R. Ramaneti, T. Banerjee, H. Gokcan, E. Haq, D. H. A. Blank, R. Jansen, and J. C. Lodder, J. Appl. Phys. **95**, 7324 (2004).
[11] N. Nakagawa, M. Asai, Y. Mukunoki, T. Susaki, and H. Y. Hwang, Appl. Phys. Lett. **86**, 082504 (2005).
[12] A. Sawa, T. Fujii, M. Kawasaki, and Y. Tokura, Appl. Phys. Lett. **86**, 112508 (2005).
[13] Z. G. Sheng, B. C. Zhao, W. H. Song, Y. P. Sun, J. R. Sun, and B. G. Shen, Appl. Phys. Lett. **87**, 242501 (2005).
[14] Z. Luo and J. Gao, J. Appl. Phys. **100**, 056104 (2006).
[15] Z. Luo, J. Gao, A. B. Djurisic, C. T. Yip, and G. B. Zhang, Appl. Phys. Lett. **92**, 182501 (2008).
[16] J. F. Wang and J. Gao, J. Appl. Phys. **109**, 07D708 (2011).
[17] P. Han, K. J. Jin, H. B. Lu, Q. L. Zhou, Y. L. Zhou, and G. Z. Yang, Appl. Phys. Lett. **91**, 182102 (2007).
[18] A. Ruotolo, C. Y. Lam, W. F. Cheng, K. H. Wong, and C. W. Leung, Phys. Rev. B **76**, 075122 (2007).
[19] T. Susaki, N. Nakagawa, and H. Y. Hwang, Phys. Rev. B **75**, 104409 (2007).
[20] J. F. Wang, Z. P. Wu, and J. Gao, J. Appl. Phys. **111**, 07D724 (2012).
[21] Y. Hikita, Y. Kozuka, T. Susaki, H. Takagi, and H. Y. Hwang, Appl. Phys. Lett. **90**, 143507 (2007).